Thermochimica Acta 621 (2015) 74–80

Contents lists available at ScienceDirect

Thermochimica Acta

journal homepage: www.elsevier.com/locate/tca

Development of pure Mg open-cell foams as structured CO_2 captor

I.A. Figueroa[a,*], M.A. Suarez[a], M. Velasco-Castro[a], H. Pfeiffer[a], B. Alcántar-Vázquez[a], G. González[a], I. Alfonso[b], G.A. Lara-Rodríguez[a]

[a] Instituto de Investigaciones en Materiales, Universidad Nacional Autónoma de México (UNAM), Circuito Exterior S/N, Cd. Universitaria, C.P. 04510 México, D.F., Mexico

[b] Instituto de Investigaciones en Materiales, Unidad Morelia, Universidad Nacional Autónoma de México, Campus Morelia UNAM, Antigua Carretera a Pátzcuaro No. 8701, Col. Ex-Hacienda de San José de la Huerta, C.P. 58190 Morelia, Michoacán, Mexico

ARTICLE INFO

Article history:
Received 6 August 2015
Received in revised form 15 October 2015
Accepted 17 October 2015
Available online 21 October 2015

Keywords:
Thermogravimetric analysis
Oxidation
Isothermal experiments
CO_2 capture
Foams

ABSTRACT

The CO_2 capture capacity of the superficial oxide layer formed in pure open-cell Mg foams was studied at low temperatures (40–60 °C) varying the relative humidity from 40 to 80%. Mg foam samples with pore size of 350 μm and surface area of 5.4 m^2/g were used for these analyses. Optical microscopy and X-ray diffraction techniques were used to characterize the cell structure and the superficial oxide formed in the cell-foams, respectively. The final products formed after the CO_2–H_2O capture experiments were identified by scanning electron microscopy and attenuated total reflexion-Fourier transform infrared spectroscopy (ATR-FTIR). The $MgCO_3$ and other products, formed after $CO_2 + H_2O$ capture process, were thermally decomposed, to quantify the amount of CO_2 captured by the superficial MgO layer using standard thermogravimetric analysis. The results showed that the highest amount of CO_2 captured was obtained at 60 °C and 80% of relative humidity, with a CO_2 capture capacity of 0.87 mmol/g, which is comparable with others CO_2 MgO-based captors. The considerable CO_2 capture capacity at low temperatures supports the potential of the pure open-cell Mg foams to be used as structured CO_2 captors.

1. Introduction

Metallic foams are a new class of materials used as impact absorbers, dust and fluid filters, heat exchangers, flame arresters, among other applications, because these materials have shown a good combination of several properties, such as high strength-to-weight ratio, high energy absorption capacity, high gas and liquid permeability, low thermal conductivity and large surface area [1–3]. The development of Mg foams has been of great interest, because these materials have shown similar functionality of Al foams but with less weight. On the other hand, Mg foams have been mainly studied for their functional properties, i.e. sound and energy absorption capacity, excellent vibration reduction capacity and lately have been recognized as promising biomaterial for bone implants [4,5].

Recently, a special emphasis has been set on studying the separation of CO_2 from the flue gases present in the ecosystem. In that sense, different kind of materials has been studied as possible CO_2 captors, such as organic sorbents [6], zeolites [7], activated carbons [8], alkaline ceramics [9], hydrotalcites [10], calcium and magnesium oxides [11,12]. These oxides powders are widely used for CO_2 capture due their wide availability, low cost, and facility of being produced in bulk amounts.

The development of structured CO_2 captors such as single piece extruded lattices, CO_2 captor coating (e.g. zeolites) over metallic substrates, and silica gel packed within aluminum foams structures, is still under study [13]. These systems offer the advantages of greater structural stability compared to the normally reported compacted powders of CO_2 captors. It is worthy of note that the techniques to develop these systems are complex and expensive.

Base on the above, to date, there are not reports on pure open-cell Mg foams used as CO_2 captors. These Mg foams, with large surface area, could be oxidized in a controlled way to form superficial Mg oxides making them attractive as structured CO_2 captors. From an engineering point of view, the open-cell Mg foams could be used, as mentioned above, in functional applications (filters, thermal and acoustic insulation, energy absorbers, etc.) and as CO_2 captors at the same time. In addition, these can be used several times if the reaction products formed after CO_2 capture process are removed.

* Corresponding author.
E-mail address: iafiguera@unam.mx (I.A. Figueroa).

http://dx.doi.org/10.1016/j.tca.2015.10.011
0040-6031/

Water steam is a very common component of flue gases emitted from different combustion process. Therefore, it is very important to analyze how the CO_2 capture is affected due its presence on the Mg oxide. The objective of the present work was to study the CO_2 capture using Mg oxide, derived from the surface oxidation of pure open-cell Mg foams. The process for CO_2 capture carry out at different relative humidities and low temperatures was also assessed.

2. Experimental procedures

2.1. Fabrication of Mg foams

Pure Mg open-cell foams were produced by the replication casting process with an atmosphere highly controlled (Ar). The porous preforms were manufactured using irregular particles of pure NaCl (<99.99%), which were sieved, separated in three average sizes and classified as (A) 350 μm, (B) 420 μm and (C) 590 μm ± 5 μm. The NaCl particles were cold pressed within the crucible to form the porous preforms. Mg ingots of commercial purity (99.5%) were placed over the preform and melted at 750 °C under a low (Ar) gas pressure (0.1 MPa). Afterwards, the NaCl preform was infiltrated with the molten metal using Ar at a pressure of 0.4 MPa, for 10 min. When the formed Mg–NaCl composite was completely solidified, this was extracted from the reactor, and then machined in order to obtain several samples for their analysis. The NaCl particles were completely dissolved in a solution of $NaOH + H_2O$. Based on the potential-pH (Pourbaix) diagram [14], it was essential to use a pH = 13, in order to avoid corrosion by pitting in the Mg matrix.

The average pore size was obtained by means of optical microscopy, where at least 100 measurements were taken for each sample. The density of the open-cell Mg foams was obtained using a pycnometer "ultrapyc 1200e" for solids, with cubic-shaped samples of ~1 cm^3. On the other hand, the percentage of porosity P (%) was calculated using the relative density δ_{Rel}. BET surface area was measured with a Bel-Japan Minisorp II equipment, employing a multipoint technique. The samples were degasified at room temperature under vacuum for 24 h before the N_2 adsorption–desorption test.

2.2. Superficial oxidation of the pure open-cell Mg foams

In order to determine the optimal superficial oxidation conditions for the Mg foams, a thermogravimetric analysis (TGA) was carried out using three different flows of oxygen (commercial purity) 20, 40 and 80 mL/min, in a temperature range from 30 to 550 °C. The oxidation tests were performed in a SDT600 instrument. Based in the TG analysis, the Mg foams were oxidized at 500 °C during 0.5, 1 and 2 h in a tubular furnace under an oxygen flow volume of 40 mL/min.

The oxidized samples were characterized by X-ray diffraction in order to determinate the kind and amount of the oxide formed on the foam surface. The comparison of relative heights method was used in the semi-quantitative XRD analysis. XRD patterns were obtained using a diffractometer D8 Advance-Bruker (with a Cu $K\alpha_1$ radiation) and correlated with the corresponding JCPDS files. Additionally, the microstructural characterization of the oxidized samples before and after CO_2 capture experiments was determined by scanning electron microscopy using a JEOL JSM-7600F. A JEM-9320 FIB instrument was used to prepare the samples for the SEM analysis.

2.3. CO_2 capture

The CO_2 capture experiments were carried out in a water vapor environment. Isothermal experiments were performed at different relative humidities (RH) (40, 60 and 80%) and temperatures of 40 and 60 °C. These experiments were performed using a temperature-controlled thermo-balance TA instrument model Q5000SA, equipped with a humidity-controlled chamber. All the experiments were realized employing distilled water and CO_2 (grade 3.0) as carrier gas. The CO_2 flow used was 100 mL/min, and the RH percentages were automatically controlled with the Q5000SA equipment.

After the isothermal experiments the samples were analyzed by Fourier transform infrared (FTIR) spectroscopy using the attenuated total reflexion (ATR) module with the aim of identifying the reaction products and then by TGA, to perform a decomposition process. The TGA experiments were performed under N_2 atmosphere, in a temperature range from 30 to 450 °C, with a heating rate of 5 °C/min using a SDT600 equipment. For the FTIR spectroscopy, the samples were analyzed on a spectrometer Alpha-Platinum (Bruker). After the decomposition process, the samples were introduced in a reagent (100 g CrO_3, 5 g $AgNO_3$, 10 g $Ba(NO_3)_2$) with the purpose of cleaning the surface area for a new oxidation process.

3. Results and discussion

3.1. Cell structure

Fig. 1 shows the structures of pure Mg open-cell foams with three pore sizes: (a) (A) 350 μm, (b) (B) 420 μm, and (c) (C) 490 μm. From these images, it can be seen that the foams have a homogeneous pore distribution with size and shape equivalent to those of the NaCl particles used as space holders. Furthermore, these results clearly showed that the foams produced have interconnected porosity, which is of great importance for the objective of this work.

The percentage of porosity Pr (%) of Mg foams was calculated using the relative density, δ_{Rel} (defined as the foam density δ^* between metal matrix density δ_{Mg} = 1.74 g/cm^3) in the following expression: Pr (%) = (1 − relative density) × 100.

Table 1 summarizes the obtained experimental parameters used to calculate the percent of porosity Pr (%). From this table, it can be seen that the Pr (%) increased as the pore size increases. On the other hand, when the pore size decreased, the relative density and the foam density also increased. This behavior has also been reported in previous works [15,16]. In the latter columns of Table 1, the values of the BET surface area and the cell-walls thickness of the foams are shown. Foams with pore size of 350 μm and relative density of 0.33 had the smallest cell-wall thickness (320 μm) and the highest surface area (5.1 m^2/g). The surface area of the sample "C" was not measured because of its pore size exceeded the measuring capacity of the equipment. Based on the above, only the sample "A" with the highest surface area was used for the CO_2 capture study.

3.2. Superficial oxidation of open-cell Mg foams

The open-cell Mg foams must be composed by a solid Mg matrix and a thin MgO layer so that it can be used as structural CO_2 captor. To set the optimal superficial oxidation parameters such as oxygen flows, temperatures, times, etc., a thermo-gravimetric analysis under an oxygen atmosphere was used (as mentioned above). Fig. 2 shows an oxidation thermogram of open-cell Mg foams under three oxygen flows. Similar oxidation behaviors at flows between 20 mL/min and 80 mL/min were observed. It was found that these oxygen flow volumes did not influence the magnitude of superficial oxidation of open-cell Mg foams. This behavior could be attributed to a total saturation of the solid–gas interface. Therefore, for this work, a flow volume of 40 mL/min was used for

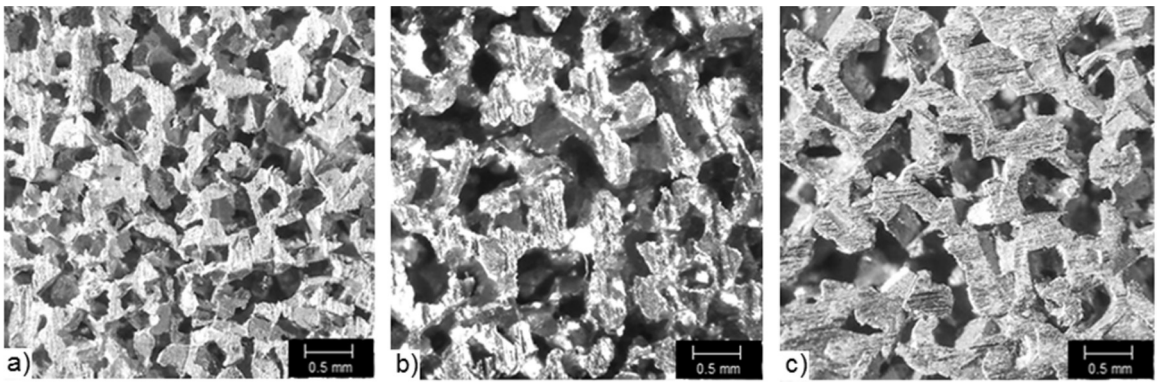

Fig. 1. Cell structure of open-cell Mg foams with different pore sizes: (a) (A) 350 μm, (b) (B) 420 μm, and (c) (C) 490 μm.

Table 1
Densities, porosities, cell-wall thickness (±10 μm) and BET surface area of open-cell Mg foams.

Sample	Density of foams, ρ^* (g/cm^3)	Relative density, ρ^*/ρ_{sMg}	Pr (%)	Surface area (m^2/g)	Average cell-thickness (μm)
(A) 350 μm	0.57	0.33	67	5.1	320
(B) 420 μm	0.47	0.27	73	4.4	370
(C) 490 μm	0.42	0.24	76	–	450

the oxidation procedure of the Mg foam samples within a tubular furnace. From the thermogram, an optimum temperature range from 475 °C to 550 °C for the oxidation of Mg foams was observed. A temperature of 500 °C was used for the oxidation of Mg foams because at higher temperatures the reactivity of Mg considerably increases. The oxidation time will be discussed later.

3.3. Identification of the phases

3.3.1. X-ray diffraction

Fig. 3 shows the XRD patterns of the Mg foams oxidized at 500 °C at different times. The diffractograms are mainly formed by the pure Mg (JCPDS file 00-004-0770) and for the MgO periclase compound (file JCPDS 01-089-4248) as it could be expected. Based on semi-quantitative XRD analysis, the amount of MgO obtained on the oxidized foams at times of 0.5 h, 1 h and 2 h were 3%, 5.5% and 8.9% (in wt.), respectively. Although, the samples heat-treated (oxidized) for 2 h showed the highest amount of MgO formation on the cell-surfaces, an analysis about its physical properties is required in order to find out the optimum thickness for such oxide layer, which could lead to the highest amount of CO_2 capture.

3.3.2. SEM characterization

The structural analysis of the superficial oxide formed on the Mg foams is essential as this will be used for the CO_2 capture. Fig. 4a shows the smooth surface of the Mg matrix before of the oxidation process, where some small oxide particles were formed. Fig. 4b shows a representative SEM-micrograph of the oxide layer formed on the surface of the open-cell Mg foams as result of oxidation process. The EDS-microanalysis carried out on the oxide layer corroborated the type of oxide (MgO, periclase) formed on the Mg foam surface (Fig. 4b inset).

The resulting MgO layer displayed large amounts of micro-porosities and micro-cracks. The micro-porosity cannot be considered as a macroscopic defect, as through such defects, gases such as CO_2, O_2 and water vapor (H_2O) can diffuse into this oxide layer, increasing the reaction area. On the other hand, these micro-cracks, which are typical of this kind of oxides, can be considered as an important defect. This defect tends to reduce its mechanical

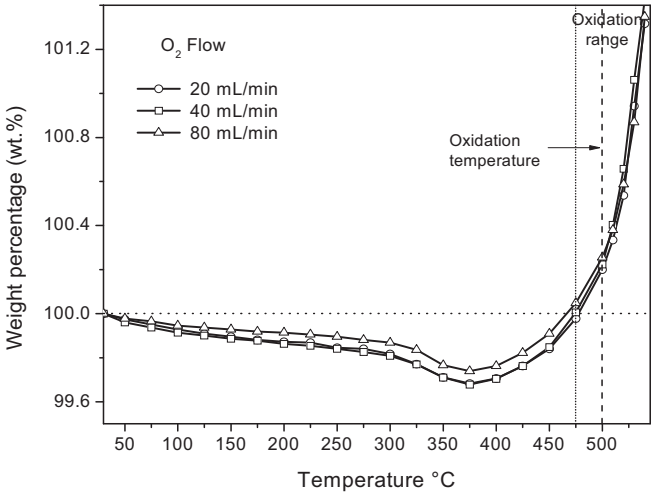

Fig. 2. Oxidation thermogram of pure open-cell Mg foams evaluated at different oxygen flow volumes.

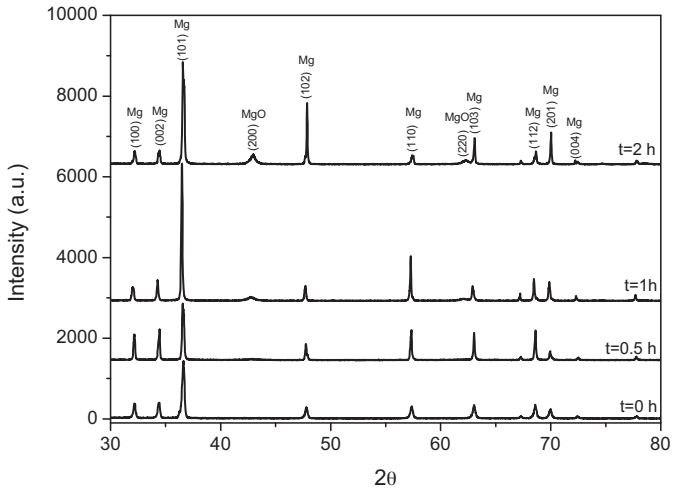

Fig. 3. X-ray diffraction patterns of pure Mg foams oxidized at 500 °C at different times.

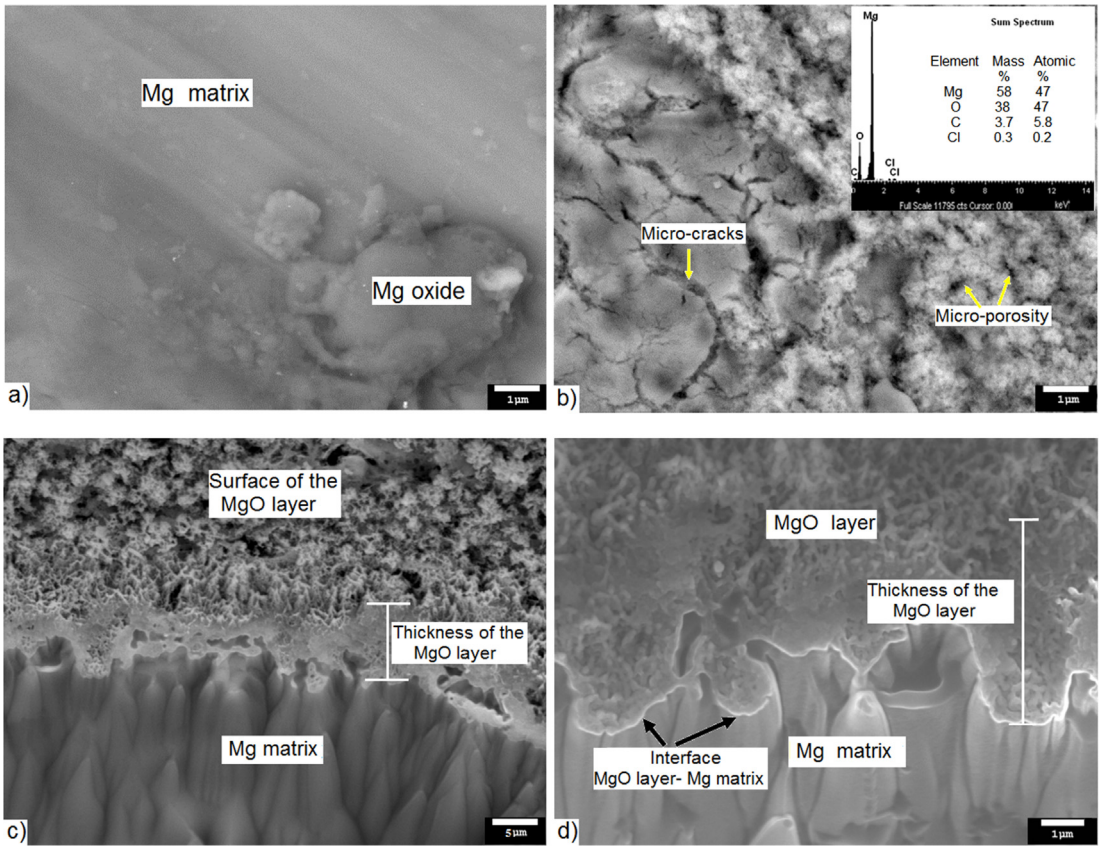

Fig. 4. (a) Surface of the Mg matrix, (b) surface layer of the MgO formed on oxidized samples (at 500 °C for 1 h), (c) cross section of the MgO layer and d) morphology of MgO.

strength and affects the adherence to the metal matrix. Therefore, the thickness of the oxide layer should be limited to a few microns in order to maintain its structural integrity.

Fig. 4c shows the cross section of the sample oxidized at 500 °C for 1 h. The thickness of the MgO oxide layer as well as the interface Mg matrix–MgO oxide layer can be clearly observed. The interconnected porosity of the foams facilitated the oxygen flow through entire material, allowing the formation of an MgO layer on the cell walls of the Mg foams. The thickness of the MgO oxide layer was characterized and measured at different parts of the sample, i.e. from the outer surface to the center of the sample. The average thickness measured of the samples oxidized at 500 °C for 0.5, 1 and 2 h were of 1 (±0.2), 6 (±2) and 14 (±2) μm, respectively. It is important to mention that the oxide layers with thicknesses between 6 and 8 μm were selected for the CO_2 capture experiments. This is due to the oxide layers with thickness higher than 14 μm presented discontinuities, produced by the fragmentation and detachment of such oxide.

Fig. 4d shows a SEM-micrograph magnification of the cross section of the MgO layer in which the structure of the MgO can be observed. The MgO layer formed on the cell-foam surface showed a kind of branched structure, uniformly distributed. Due to this branched structure, the surface texture of the oxide layer ended very rough.

3.4. Capture of CO_2

In order to determine the CO_2 capture capacity of the MgO layer formed on the surface of the open-cell Mg foams several isothermal experiments were conducted. The CO_2–H_2O capture experiments were carried out at low temperatures (40 °C and 60 °C) and different relative humidities (40–80%) using a CO_2 flow of 100 mL/min and MgO weight of about 1.06 mg. This weight corresponds to the oxide layer formed on the surface of cubic shaped Mg foam samples (with an average volume of 0.064 cm^3 and a weight of 36.5 mg), which was measured by means of TG analysis at a constant temperature of 500 °C, using a O_2 flow of 40 mL/min for 1 h.

Fig. 5a shows the isotherms performed at a temperature of 40 °C and relative humidities of 40, 60 and 80%. From these curves, it can be observed that most of the CO_2–H_2O capture process occurs during the first 40 min and the process reaches almost its equilibrium (saturation point) at ~60 min. In addition, the CO_2–H_2O capture capacity increased as relative humidity increases. The maximum weight gain of 3.4% was obtained for the sample tested at 80% RH, after 180 min of reaction.

Fig. 5b shows the isotherms evaluated at the highest temperature (60 °C) with the same relative humidity range. At this temperature, most of the CO_2–H_2O capture process took place during the first 70–80 min, and 10 min after, it seems to reach the equilibrium stage. At this temperature, the largest increment in weight was observed, recording a maximum increment of 5.8 wt% for the sample evaluated with 80% RH, after 180 min of reaction. The initial times for the CO_2–H_2O capture process obtained in the isotherms are slightly longer when compared with other CO_2 capture systems (commonly powders) [17,18]. A plausible explanation to this can be attributed to the partly porous structure of the oxide layer as well as its textural properties (surface area, porosity, etc.).

From the above, in general, these results suggested that the increments in temperature and relative humidity increased the CO_2–H_2O capture capacity of the MgO layer. From the literature, the following sequential reaction mechanism for the CO_2–H_2O capture on MgO was reported [19].

$$Mg(s) + ½O_2(g) \rightarrow MgO(s) \quad (1)$$

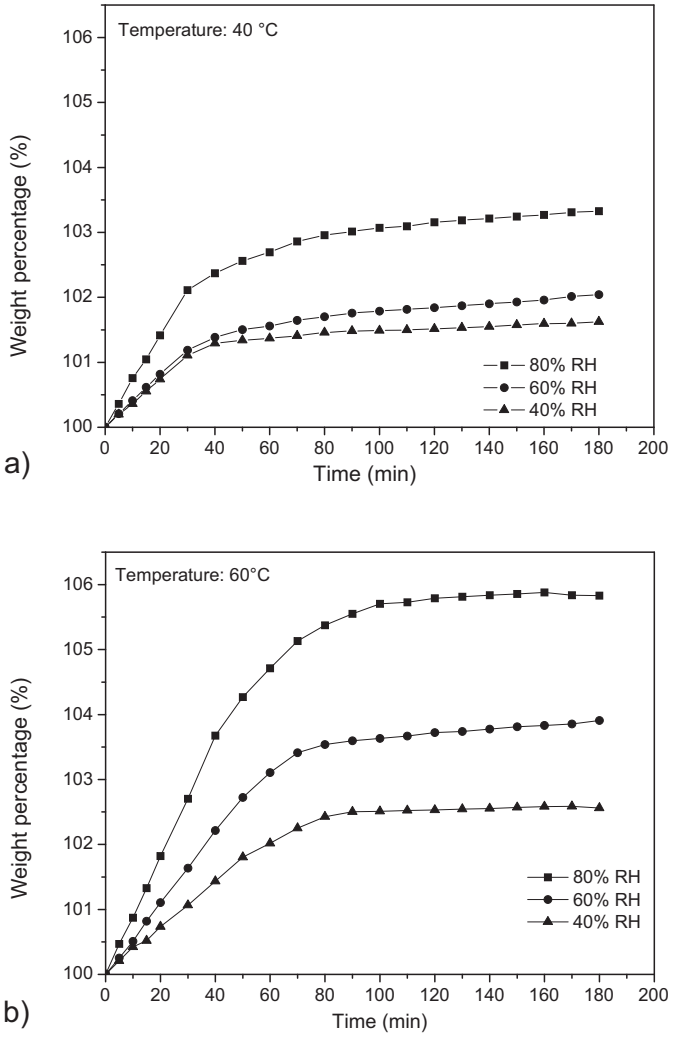

Fig. 5. Isotherms of CO_2–H_2O capture on Mg foams (oxidized at 500 °C for 1 h) varying the relative humidity at 40, 60 and 80% and temperatures of (a) 40 °C and (b) 60 °C.

$$MgO(s) + H_2O(v) \rightarrow Mg(OH)_2(s) \quad (2)$$

$$Mg(OH)_2(s) + CO_2(g) \rightarrow MgCO_3(s) + H_2O(v) \quad (3)$$

In this sequential reaction mechanism, the steam water initially reacts with MgO to produce $Mg(OH)_2$, reaction (2). Then, as the $Mg(OH)_2$ is more reactive to CO_2 than MgO, the CO_2 capture is increased, obtaining $MgCO_3$ plus H_2O as final products, reaction

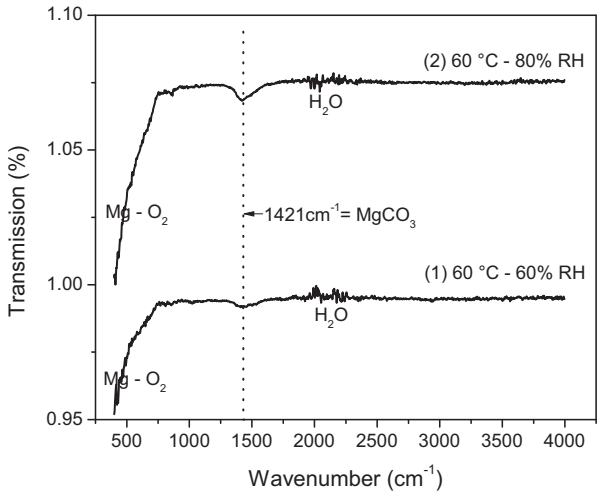

Fig. 7. Infrared spectra of Mg foam samples after CO_2–H_2O capture process.

(3). The H_2O acts as catalytic active specie, which does modify the activation energy value of the whole reaction process. The nature of this CO_2 capture reaction (3) is exothermic, with a ΔH value of −19.7 kJ/mol of CO_2. This means that the heat required for the regeneration of the reverse reaction to form $Mg(OH)_2$ is lower, as reported in Ref. [20]. Therefore, the CO_2 capture reaction (3) can be carried out in several cycles. The Gibbs energy (ΔG) calculated for the capture reaction (3) was −12.69 kJ, therefore, the reaction could be considered as spontaneous, considering the reaction mechanism established in Eq. (3). A looping study for carbonation and de-carbonation of the reported material is in process and will be reported elsewhere.

In order to experimentally identify and quantify the final products obtained after the CO_2–H_2O capture experiments, the samples were analyzed by means of the SEM-EDS, TGA and FTIR techniques. It is worthy of note that due to the size of the sample used for the CO_2–H_2O capture experiments, it was not possible to use XRD technique, therefore, the FTIR technique was employed.

Fig. 6a shows an elemental mapping of elements and Fig. 6b shows a global SEM-EDS analysis carried out on the carbonated surface of Mg foams samples. The elemental mapping analysis showed a homogeneous distribution of the elements Mg, C and O. On the other hand, the global quantification of elements, i.e. Mg (22%), C (21%), O (56%), and traces (1%) in at%, indicated the formation of the $MgCO_3$ compound after the CO_2–H_2O capture process. The original branched morphology of the MgO shown in Fig. 4 was retained after this CO_2–H_2O capture process.

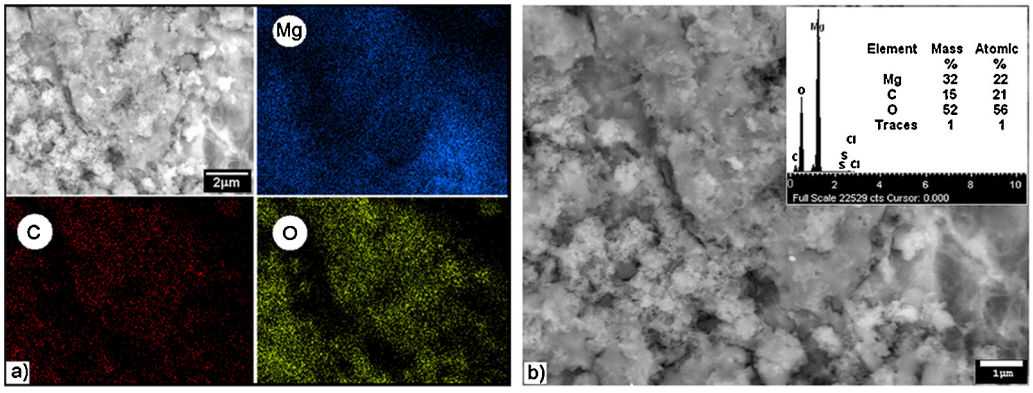

Fig. 6. (a) Distribution of elements (mapping) and (b) global SEM-EDS analysis of a selected section of the MgO layer after the CO_2–H_2O absorption process.

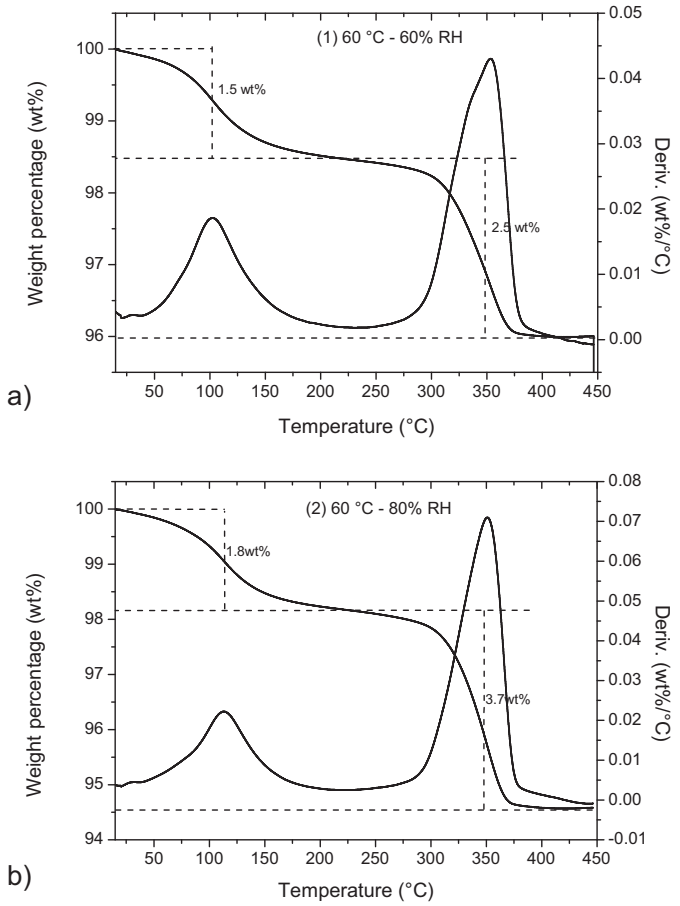

Fig. 8. TG and DTG curves of the samples treated at 60 °C and relative humidities of: (a) 60% RH and (b) 80% HR.

Fig. 7 shows the FTIR results performed on two samples (those with the highest weight gain) obtained from the isothermal experiments at 60 °C and 60% RH (1) and 80% RH (2). In both infrared spectra, a wide vibration band centered at 1421 cm^{-1} was observed, that corresponded to the $MgCO_3$ vibration. Besides, vibrations due to the presence of Mg-oxygen and H_2O, were also detected at wavenumber intervals of 400–750 and 1800–2300 cm^{-1}, respectively. The reported signals for those components using FTIR agree well with those reported in the literature [21,22]. Besides, these results are also in agreement with the reaction mechanism for the CO_2–H_2O capture mentioned above.

The $MgCO_3$ formed during the CO_2–H_2O capture process was thermally decomposed to quantify the amount of CO_2 and H_2O captured by the MgO layer using a standard TG analysis. Fig. 8(a) and (b) shows two thermograms performed at 5 °C per minute on the samples treated at (a) 60 °C – 60% RH and (b) 60 °C – 80% RH. In these thermograms, a total weight loss of 4 wt% and 5.5 wt% were obtained for the samples (1) 60 °C – 60% RH and (2) 60 °C – 80% RH, respectively. The weight losses are attributed to dehydration and decarbonation processes.

The first drop in weight observed in the TG curves between room temperature and 200 °C is due to the dehydration process. Samples 60 °C – 60% RH (1) and 60 °C – 80% RH (2) lost 1.5 and 1.8 wt%, respectively. According to the reaction proposed by James C. Fisher et al., the $MgCO_3$ carbonate can be decomposed between 375 and 400 °C and release CO_2 [23]. Therefore, the second drop in weight observed in the thermograms (between 300 and 400 °C) corresponded to the CO_2 capture capacity with values of 2.5 and 3.7 wt%, equivalent to 0.58 mmol/g, and 0.87 mmol/g for samples (1) and (2), respectively. Please note that the CO_2 capture capacities are comparable with others MgO based powder systems studied for the CO_2 capture [24,25]. Should the increment of CO_2 capture capacity of the Mg is required; the increment of MgO layer and/or by coating its superficial area with alkaline metals could be highly advisable.

It is worth mentioning that the lack of adherence of the $MgCO_3$ layer formed after the CO_2–H_2O capture is considered in this work as beneficial, as when the cyclic CO_2–H_2O capture capacity of the MgO decreases, this layer can be chemically or mechanically removed and the formation of a new MgO layer will be possible. Considering the thickness of the cell-foams (320 μm) and the MgO oxide layer (6–8 μm), the Mg foams under study could be used at least 10 times keeping the strength of the metallic structure. It should also be borne in mind that the material reported in this work could, easily, withstand the stresses (tensile-compressive) produced by the change of volume of the formed ceramic-based layer used to capture the CO_2. On this basis, if we start with foams produced with pure MgO, as soon as the capture CO_2 capture takes place, the change in volume that occurs during the reaction to produce $MgCO_3$ will embrittle the MgO foam, cracking and crumbling it apart, and therefore, limiting the engineering application of this and any other CO_2 captor ceramic-based powders. Besides, with the process reported here, it is possible to produce metallic foams from rather small samples to several dozens of millimeters.

4. Conclusions

The CO_2 capture capacity of the pure open-cell Mg foams depends of several factors such as (1) cell structure, pore size, percentage of porosity and surface area, (2) amount of the MgO formed on the foam surface, and (3) CO_2–H_2O capture process variables, such as temperature and relative humidity (RH). The MgO layers (with thicknesses between 6 and 8 μm) formed on the Mg foams with pore size of 350 μm showed the maximum CO_2 capture capacity (0.87 mmol/g) at 60 °C and 80% RH. This considerable CO_2 capture capacity of the pure open-cell Mg foams at low temperatures opens the possibility of using them as structured CO_2 captors. The development of pure open-cell Mg foams as structured CO_2 captors does not require complex processing techniques; therefore, the open-cell Mg foams can be used for the separation of carbon dioxide from environmental fulfilling their functional applications and with the possibility to be reused several times. In addition, the ultra-lightweight porous structure of these Mg foams can be coated with other CO_2 captor materials and increase this capture capacity. Therefore, the coating of the superficial area with alkaline metals could be highly advisable if the increment of CO_2 capture capacity of the Mg foam is required.

Acknowledgements

The authors would like to acknowledge the financial support from SENER–CONACYT 151496 for funding the project. C. Flores, O. Novelo, J. Romero, A. Tejeda, J. Morales, E. Sánchez, E. Hernández-Mecinas, J.M. Garcia and F. Garcia are also acknowledge for their technical support. “Por mi raza hablará el espíritu”.

References

[1] J. Banhart, Manufacture, characterization and application of cellular metals and metal foams, Prog. Mater. Sci. 46 (2002) 559.
[2] L.J. Gibson, Mechanical behavior of metallic foams, Annu. Rev. Mater. Sci. 30 (2000) 191–227.
[3] H.P. Degischer, in: H.P. Degischer, B. Kriszt (Eds.), Handbook of Cellular Materials Production, Processing, Applications, Wiley-VCH, Weinheim, 2002, pp. 5–7.

[4] D.H. Yang, B.Y. Hur, S.R. Yang, Study on fabrication and foaming mechanism of Mg foam using $CaCO_3$ as blowing agent, J. Alloys Compd. 461 (2008) 221–227.
[5] M.P. Staiger, A.M. Pietak, J. Huadmai, G. Dias, Magnesium and its alloys as orthopedic biomaterials: a review, Biomaterials 27 (2006) 1728–1734.
[6] R. Maceiras, S.S. Alves, M.A. Cancela, E. Alvarez, Effect of bubble contamination on gas–liquid mass transfer coefficient on CO_2 absorption in amine solutions, Chem. Eng. J. 137 (2008) 422–427.
[7] E. Diaz, E. Muñoz, A. Vega, S. Ordoñez, Enhancement of the CO_2 retention capacity of Y-zeolites by Na and Cs treatments: effect of adsorption temperature and water treatment, Ind. Eng. Chem. Res. 47 (2008) 412–418.
[8] C. Pevida, M.G. Plaza, B. Arias, H. Fermoso, F. Rubiera, J. Pis, Surface modification of activated carbons for CO_2 capture, Appl. Surf. Sci. 254 (2008) 7165–7172.
[9] B.N. Nair, R.P. Burwood, V.J. Goh, K. Nakagawa, T. Yamaguchi, Lithium based ceramic materials and membranes for high temperature CO_2 separation, Prog. Mater. Sci. 54 (2009) 511–541.
[10] E.L.G. Olvera, C.A. Grande, A.E. Rodrigues, CO_2 sorption on hydrotalcite and alkali-modified (K and Cs) hydrotalcites at high temperatures, Sep. Purif. Technol. 62 (2008) 137–147.
[11] D.Y. Lu, R.W. Hughes, E.J. Anthony, V. Manovic, Sintering and reactivity of $CaCO_3$ based sorbents for in situ CO_2 capture in fluidized beds under realistic calcinations conditions, J. Environ. Eng. 135 (2009) 404–410.
[12] S.C. Lee, H.J. Chae, S.J. Lee, B.Y. Choi, C.K. Yi, J.B. Lee, C.K. Ryu, J.C. Kim, Development of regenerable MgO based sorbent promoted with K_2CO_3 for CO_2 capture at low temperatures, Environ. Sci. Technol. 42 (2008) 2736–2741.
[13] J. Knox, D. Howard, J. Perry, Engineered structured sorbents for the adsorption of carbon dioxide and water vapor from manned spacecraft atmosphere: applications and modeling 2007/2008, in: International Conference of Environmental Systems, 2008, 01-2094.
[14] A. Shaw Barbara, Corrosion resistance of magnesium alloys ASM Handbook, Corrosion: Fundamentals, Testing, and Protection (#06494G), 13A, 2003, pp. 694.
[15] J. Trinidad, I. Marco, G. Arruebarrena, J. Wendt, D. Letzig, E. Sáenz de Argandoña, R. Goodall, Processing of magnesium porous structures by infiltration casting for biomedical applications, Adv. Eng. Mater. 16 (2014) 241–247.
[16] J.O. Osorio-Hernández, M.A. Suarez, R. Goodall, G.A. Lara-Rodriguez, I. Alfonso, I.A. Figueroa, Manufacturing of open-cell Mg foams by replication process and mechanical properties, Mater. Des. 64 (2014) 136–141.
[17] M.K. Ram Reddy, Z.P. Xu, G.Q. (Max) Lu, J.C. Diniz da Costa, Influence of water on high-temperature CO_2 capture using layered double hydroxide derivates, Ind. Eng. Chem. Res. 47 (2008) 2630–2636.
[18] L. Martinez-dlCruz, H. Pfeiffer, Microstructural thermal evolution of the Na_2CO_3 phase produced during a Na_2ZrO_3–CO_2 chemisorption process, J. Phys. Chem. C 116 (17) (2012) 9675–9680.
[19] S. Wang, S. Yan, X. Ma, J. Gong, Recent advances in capture of carbon dioxide using alkali-metal-based oxides, Energy Environ. Sci. 4 (2011) 3805.
[20] R.V. Siriwardane, R.W. Stevens, Novel regenerable magnesium hydroxide sorbents for CO_2 capture at warm gas temperature, Ind. Eng. Chem. Res. 48 (2009) 2135–2141.
[21] K. Nakamoto, Infrared Raman Spectra of Inorganic and Coordination Compounds, Wiley, 2009.
[22] F.A. Miller, C.H. Wilkins, Anal. Chem. 24 (1952) 1253.
[23] J.C. Fisher, R.V. Siriwardane, $Mg(OH)_2$ for CO_2 capture from high-pressure, moderate-temperature gas streams, Energy Fuels 28 (2014) 5936–5941.
[24] M. Bhagiyalakshmi, J.Y. Lee, H.T. Jang, Synthesis of mesoporous magnesium oxide: its application to CO_2 chemisorption, Int. J. Greenh. Gas Control 4 (2010) 51–56.
[25] M. Bhagiyalakshmi, P. Hemalatha, M. Ganesh, P.M. Mei, H.T. Jang, A direct synthesis of mesoporous carbon supported MgO sorbent for CO_2 capture, Fuel 90 (2011) 1662–1667.